DTIC FILE COPY (2)

AD-A203 469

# DOCUMENTATION PAGE

Form Approved OMB No. 0704-0188

| | |
|---|---|
| UNCLASSIFIED | 1b. RESTRICTIVE MARKINGS |
| 2a. SECURITY CLASSIFICATION AUTHORITY | 3. DISTRIBUTION/AVAILABILITY OF REPORT<br>Approved for public release; distribution is unlimited. |
| 2b. DECLASSIFICATION/DOWNGRADING SCHEDULE | |
| 4. PERFORMING ORGANIZATION REPORT NUMBER(S)<br>AFAL-TR-88-114 | 5. MONITORING ORGANIZATION REPORT NUMBER(S) |
| 6a. NAME OF PERFORMING ORGANIZATION<br>Air Force Astronautics Laboratory<br>6b. OFFICE SYMBOL (If applicable) RKPA | 7a. NAME OF MONITORING ORGANIZATION |
| 6c. ADDRESS (City, State, and ZIP Code)<br>Edwards AFB CA 93523-5000 | 7b. ADDRESS (City, State, and ZIP Code) |
| 8a. NAME OF FUNDING/SPONSORING ORGANIZATION<br>8b. OFFICE SYMBOL (If applicable) | 9. PROCUREMENT INSTRUMENT IDENTIFICATION NUMBER |
| 8c. ADDRESS (City, State, and ZIP Code) | 10. SOURCE OF FUNDING NUMBERS |

| PROGRAM ELEMENT NO. | PROJECT NO. | TASK NO | WORK UNIT ACCESSION NO. |
|---|---|---|---|
| 62302F | 5730 | 05 | NK |

11. TITLE (Include Security Classification)
Viscoelastic Response and Adhesion Properties of Highly Filled Elastomers (U)

12. PERSONAL AUTHOR(S)
Stacer, Ross G., Husband, David M., and Stacer, Heidi L.

| 13a. TYPE OF REPORT | 13b. TIME COVERED | 14. DATE OF REPORT (Year, Month, Day) | 15. PAGE COUNT |
|---|---|---|---|
| Special | FROM 86/1 TO 86/12 | 87/5 | 18 |

16. SUPPLEMENTARY NOTATION
This paper was published by Rubber Chemistry and Technology, Vol 60, No 2, May-June 1987, pp 227-244.

| 17. COSATI CODES | | | 18. SUBJECT TERMS (Continue on reverse if necessary and identify by block number) |
|---|---|---|---|
| FIELD | GROUP | SUB-GROUP | Viscoelasticity, Solid Propellants, Elastomers, Strain Dependence, Resilience, Master Curves, Adhesion. |
| 21 | 09 | 2 | |

19. ABSTRACT (Continue on reverse if necessary and identify by block number)

The viscoelastic response of four highly-filled elastomers has been investigated. Small deformation dynamic testing of these materials reveals that they are nonlinear viscoelastic, as well as thermorheologically complex. Nonlinear viscoelastic behavior was observed as a pronounced strain dependence in the range of 0.1 to 10%. The degree of this nonlinear response was quantified through a constitutive equation containing a single nonlinear factor; resultant nonlinear factors for the various materials were comapred and evaluated. Thermorheologically complex behavior was displayed by slightly different shift coefficients to superpose G' and G" data. An approach for calculating material resilience from the viscoelastic data was also developed and a nomographic technique presented for its application.

A composite adhesive joint, consisting of two layers of a filled NBR compound bonded together by a filled putty interlayer, was also studied. It was found that both the adhesive fracture energy and the effect of interlayer thickness could be related to the loss modulus of the putty interlayer. FInally, the effect of contact time on bond strength was evaluated.

| | |
|---|---|
| 20. DISTRIBUTION/AVAILABILITY OF ABSTRACT<br>☒ UNCLASSIFIED/UNLIMITED ☐ SAME AS RPT. ☐ DTIC USERS | 21. ABSTRACT SECURITY CLASSIFICATION<br>UNCLASSIFIED |
| 22a. NAME OF RESPONSIBLE INDIVIDUAL<br>David M. Husband, CAPT, USAF | 22b. TELEPHONE (Include Area Code) (805) 275-5534 / 22c. OFFICE SYMBOL RKPA |

DD Form 1473, JUN 86 Previous editions are obsolete. SECURITY CLASSIFICATION OF THIS PAGE

Block 19 (continued): and results presented as a master curve of adhesive fracture energy vs. temperature-reduced contact time.

Accession For
NTIS GRA&I ☒
DTIC TAB ☐
Unannounced ☐
Justification
By
Distribution/
Availability Codes
Dist | Avail and/or Special
A-1 | 20

DTIC COPY INSPECTED 4

Reprinted from RUBBER CHEMISTRY AND TECHNOLOGY,
Vol. 60, No. 2, May-June 1987
Printed in U.S.A.

# VISCOELASTIC RESPONSE AND ADHESION PROPERTIES OF HIGHLY FILLED ELASTOMERS*

R. G. STACER, D. M. HUSBAND, AND H. L. STACER

AIR FORCE ROCKET PROPULSION LABORATORY, EDWARDS AFB, CALIFORNIA 93523

## INTRODUCTION

Laboratory characterization and evaluation of highly filled elastomers for practical structural applications requires understanding several complicating factors introduced by the presence of filler. Among these are:

1) in addition to being temperature and rate sensitive, filled materials are usually strain-dependent, making their response nonlinear viscoelastic[1-3];

2) the presence of filler appears to change the temperature dependence of the dominant viscoelastic mechanism as indicated by changes in the free volume constants[4,5];

3) for filled materials, test sample size must be selected to minimize local behavior of the largest particulate inclusion[6]; and the effects of polymer-rich surfaces on molded specimens must be considered[6-8];

4) in the vicinity of filler particles, dewetting or cavitation may occur at strains far below those necessary to cause rupture[9,10]; and

5) filled specimens are sensitive to damage from previous testing or from sample preparation which may either be temporary, such as recovery from small-deformation dynamic tests[11], or permanent in nature, such as strain-induced anisotropy[12]. Each of these factors can bias laboratory evaluation by introducing experimental abnormalities. Additionally, they may severely hamper data interpretation by limiting the applicability of potentially useful techniques such as the method of reduced variables[13].

Because of these complicating factors, much of the research conducted on elastomers has employed unfilled or model-filled systems, leading to uncertainty in applying the results for these cases to filled products of practical interest. Research on small-deformation response properties has been conducted using selected filler types. Carbon black has been evaluated extensively to determine its influence on the modulus[14,15] and dynamic properties[3] of elastomers. Less attention has been focused on the behavior of nonreinforcing fillers, although two recent reviews are noteworthy[16,17]. Few accomplishments have been reported regarding the role of filler in elastomeric adhesives and adherends. Rubber-based adhesives are often compounded with filler in a similar fashion to other rubber products[18]. Results of tests to evaluate filler reinforcing action and bonded interface failure properties follow rules established for bulk failure[19]. To our knowledge, however, no systematic

* Presented at a meeting of the Rubber Division, American Chemical Society, Atlanta, Georgia, October 7-10, 1986. This paper is the work of the U.S. Government and is not, therefore, subject to U.S. copyright. B.



89 1 05 045

study has been performed to develop quantitative relationships between elastomeric interface failure properties and filler variables such as size, shape, morphology, and chemisorption.

The purpose of this paper is to characterize and evaluate the viscoelastic response and adhesion properties of a series of highly filled elastomers typically used in solid rocket motors. These include an insulating material, O-ring seal, solid propellant, and putty used in conjunction with the insulation. Small deformation dynamic properties are considered for all of these materials, as well as the adhesive strength of the insulation/putty bond and its relationship to viscoelastic dissipation.

## EXPERIMENTAL

Table I lists the primary ingredients of the materials evaluated. They represent the wide variety of elastomers used in structually critical regions of solid rocket motors and contain several common fillers, both reinforcing and nonreinforcing. The insulation is based on a high nitrile content nitrile–butadiene rubber (NBR) and is filled with both asbestos fiber and a reinforcing silica. A blended fluorocarbon binder, along with a large particle size, thermal carbon black, is used to compound the O-ring material. Energetic fillers in the liquid-polybutadiene-based propellant include an oxidizer, ammonium perchlorate (in equal percentages of 25 and 200 $\mu$m particles), and a fuel, 6 $\mu$m aluminum powder. The high tack, uncrosslinked putty consists of a polyester resin, asbestos fiber, and various pigments.

Both the as-received putty and a conditioned putty were tested to assess the influence of moisture on this material. The putty samples were conditioned at constant 88% humidity in a dessicator above a sulfuric acid solution. The samples were removed for testing once an equilibrium in weight (approximately 3%) was reached after 4 days.

TABLE I

MATERIALS FORMULATIONS

| | Material | | | |
|---|---|---|---|---|
| | Insulation[a] | O-Ring[a] | Propellant | Putty[a] |
| Filler content, (%)[b] | 38 | 22 | 86 | 43 |
| Filler(s) | Asbestos (19%) | N990 | Ammonium perchlorate (68%) | Asbestos (31%) |
| | Hi-Sil (19%) | | Al (18%) | Pigments (12%) |
| Binder | NBR Hycar 1052 | Blended Viton/Fluorel | ARCO R45M | Poly(ester) Cardill 8621 |
| Cure system | Sulfur | MgO $Ca(OH)_2$ | IPDI[c] | — |
| Manufacturer | Kirkhill | Parker | AFRPL | Randolph |

[a] Material and formulations courtesy of Morton–Thiokol.
[b] All percentages by weight.
[c] Isophorone diisocyanate.

Dynamic mechanical properties of the materials were measured using a Rheometrics Mechanical Spectrometer, Model 605. Measurements were made in forced dynamic shear using one of the three geometries shown in Figure 1, depending on the specific material. The O-ring test specimen, shown in Figure 1a, was affixed between 25 mm parallel plates by drilling 7 mm diameter holes through the center of the plates and bonding the sample securely to the two plates. A specimen length-to-diameter ratio of approximately 1.5 was used. End effects were minimal for this specimen; this was verified using three other different length samples. Small 4 mm discs of the putty were tested between parallel plates as illustrated in Figure 1b. Measurements on the insulation and propellant were conducted using a torsion 60 mm × 14 mm × 7 mm rectangular sample (Figure 1c).

Each material was first tested at a constant temperature and frequency over a range of strain levels. The glass transition temperature, $T_g$, was then determined for the three crosslinked rubbers by measuring viscoelastic dissipation as a function of temperature. $T_g$ was estimated as the temperature at which the shear loss modulus, $G''$, maximized. Finally, the viscoelastic properties were measured through four decades of frequency over a wide range of temperatures.

Insulation/putty adhesive joints were prepared as follows. Strips of NBR insulation, 5 mm thick and 10 mm wide, were bonded to steel shims of the same width using contact cement. These strips served as the substrate of the final composite joint samples. Putty was pressed to the desired thickness between plastic sheets at 0.5 MPa, then placed in a freezer at −15°C. While still cold, putty was cut into 10 mm wide strips, separated from the plastic sheets, and lightly applied to release paper. A backing strip of NBR insulation, 1 mm thick, was then placed above the putty. After the putty, NBR insulation backing, and substrate strips had all warmed to room temperature, a composite joint consisting of insulation/putty/insulation layers was pressed for one minute at 0.5 MPa. Excess putty was trimmed from the composite joint, and an average putty thickness was determined to be approximately 0.25 mm by weight differences. Samples were allowed to sit under light pressure for one day at room temperature before testing to ensure equilibrium contact conditions.

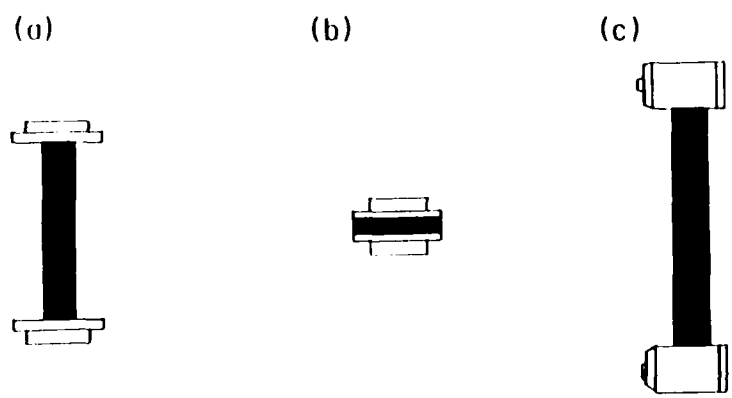


FIG. 1—Dynamic test specimens; (a) parallel plate, cylindrical mode; (b) parallel plate, disc mode; and (c) torsion rectangular.

In addition to preparing joints with constant putty thickness and contact conditions, other samples were prepared to evaluate the effect of these variables on bond strength. Different putty thicknesses were obtained by applying more than one layer of putty during joint build-up. Contact conditions were compared by evaluating samples prepared at different temperatures and monitoring changes in their adhesive strength with time at each temperature.

Adhesive joints prepared as described were placed in an Instron tensile testing device and the backing material peeled from the substrate at a 180° angle. The adhesive fracture energy, $G_a$, under these conditions is given through an energy balance approach by[20]

$$G_a = 2P/w,$$

where $P$ is the peel force and $w$ is the width of the specimen.

## RESULTS AND DISCUSSION

### NONLINEAR VISCOELASTIC RESPONSE

Figure 2 shows the dependence of shear storage modulus, $G'$, on strain amplitude for the materials. The logarithm of storage modulus decreases linearly with the logarithm of increasing shear strain level, indicating some form of damage function exists which increases with deformation. Similar behavior was exhibited by the loss modulus. This phenomenon of strain-dependent material properties, termed nonlinear viscoelastic behavior, is often associated with the presence of filler particles[2,3,13,15]. As previously mentioned, small deformation modulus measurements

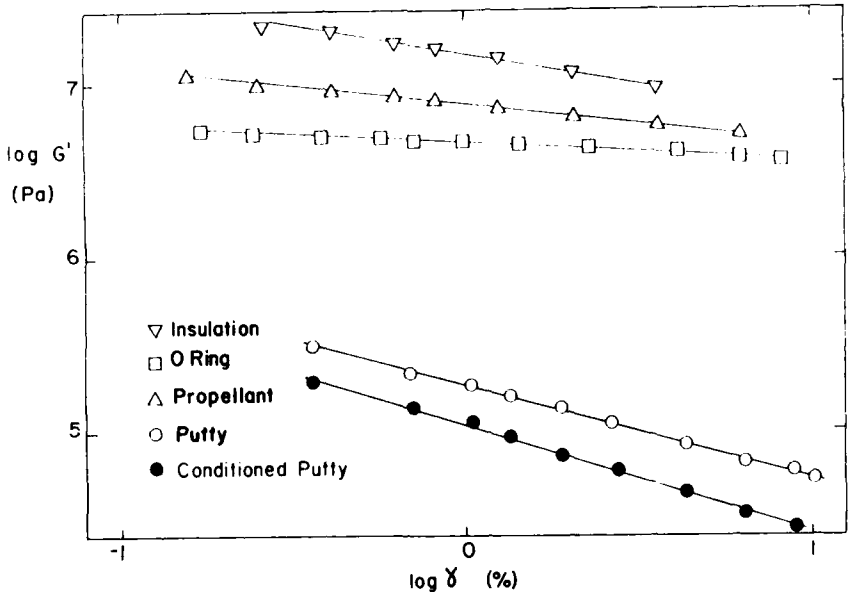


FIG. 2.—Effect of strain amplitude on shear storage modulus, $G'$, for five materials as indicated. Frequency = 1.6 $s^{-1}$, temperature = 25°C.

for filled elastomers are very sensitive to deformation history. For this reason, each test must be conducted on a virgin sample, or sufficient time allowed between successive measurements on a single sample to allow the modulus to return to its original value. This second approach was used to obtain the data in Figure 2. It was found that it took approximately 15 min of recovery time for the materials used in this study to reheal. Using this method, data were found to be highly reproducible for cycles of increasing or decreasing strain amplitude. Gui and coworkers[21] have discussed in detail dynamic modulus recovery time and the effect of strain history on the shape of modulus *vs.* strain-level curves for carbon-black-filled SBR compounds.

The general shape of modulus *vs.* strain-amplitude curves has been found to be sensitive to filler volume fraction[1], temperature and frequency[2], filler type[22], and elastomer type[23]. Payne[1], using a reinforcing carbon-black-filled natural rubber tested over four logarithmic decades of strain amplitude, showed s-shaped curves for $G'$, with plateaus at both extremes in amplitude when high filler fractions were used. These curves gradually decayed to linear relationships as filler fraction was decreased. Over a narrower range of strain, Ulmer and coworkers[22] found monotonically increasing curves as amplitude decreased for high-structure-carbon-black-filled elastomers, but near linear behavior for low-structure filler.

Data in Figure 2, representing materials utilizing predominately nonreinforcing filler, show that the logarithm of modulus is linearly dependent on strain over approximately 1.5 decades of strain. This suggests that over the strain range examined in this work, constitutive relationships can be developed of the form

$$G' = A\gamma^m \tag{2}$$

and

$$G'' = B\gamma^n, \tag{3}$$

where $A$ and $B$ are the shear storage and loss moduli at 1% strain, respectively, $\gamma$ is the strain amplitude, and the exponents $m$ and $n$ are factors representing the degree of nonlinear response. Payne[24] previously normalized shear storage modulus using the equation

$$Z = (G' - G'_\infty)/(G'_0 - G'_\infty), \tag{4}$$

where $G'_\infty$ and $G'_0$ are the plateau storage moduli at the high and low strain limits, respectively. Application of this normalization procedure was not possible in this study, since neither $G'_0$ nor $G'_\infty$ were available.

Table II lists the factors obtained by fitting the data in Figure 2 using Equation (2), and similarly for $G''$ using Equation (3). Agreement between these equations and the data is excellent as indicated by the linear regression correlation coefficients, $r^2$, given in the table. For all materials except the propellant, the absolute value of $m$ is greater than $n$. Relative values of these nonlinear factors are most likely dependent on the region of strain investigated. The origin of the strain dependence of both $G'$ and $G''$ is usually discussed in terms of the same physical mechanism. Fletcher and Gent[25] have postulated that the slope of strain-amplitude dependence of the storage modulus is related to the bond strength within the secondary filler structure. Using a similar physical picture, Payne[2] has discussed the $G''$ dependence in terms of breakdown and reformation of this structure.

TABLE II

NONLINEAR FACTORS AND REFERENCE MODULI

| Material | $m$, Pa | log $A$, Pa | $r^2$ | $n$, Pa | log $B$, Pa | $r^2$ |
|---|---|---|---|---|---|---|
| Insulation | −0.288 | 7.150 | 0.99 | −0.138 | 6.617 | 0.97 |
| O-Ring | −0.093 | 6.642 | 0.99 | −0.049 | 5.860 | 0.98 |
| Propellant | −0.121 | 6.800 | 0.97 | −0.191 | 6.446 | 0.99 |
| Putty | −0.518 | 5.256 | 0.99 | −0.368 | 5.273 | 0.99 |
| Conditioned putty | −0.630 | 5.045 | 0.99 | −0.540 | 4.971 | 0.99 |

The conditioned putty material displays the greatest nonlinear behavior (largest absolute values of $m$ and $n$). In addition to plasticizing the putty, high humidity conditioning appears to increase the nonlinear behavior. The degree of nonlinearity of the two putty compounds is similar in magnitude to that reported for high-structure-carbon-black-filled elastomers[1,22,23]. All three of the crosslinked rubbers display significantly lower absolute values of $m$ and $n$ than the putty does. This may be attributable to the asbestos fiber and pigment fillers used in the polyester putty, rather than to its uncrosslinked nature (or lower modulus). Justification for this conclusion comes from two previous studies[25,26] that reported no effect of crosslinking or crosslink density on nonlinear response.

Of all the materials studied, the O-ring displayed the lowest strain level dependence. Its nonlinear factors are near zero, close to an order of magnitude lower (in absolute value) than those determined for the putty. This is probably due to the nonreinforcing nature of the N990 black used in the O-ring formulation. A previous study using this low-structure black in natural rubber compounds showed the storage modulus was nearly independent of strain amplitude[22].

## VISCOELASTIC SPECTRUM

An example of the small deformation response properties measured for each of the materials is presented in Figure 3. This figure shows the effect of temperature and frequency on the shear loss modulus of the putty. Data were collected over three decades of logarithmic frequency and at temperatures ranging from 22 to −33°C. Loss modulus increases in a regular fashion with increasing frequency or decreasing temperature, suggesting that time–temperature superposition of the data may be possible. Similar results were obtained for each of the materials investigated, although the temperature range varied somewhat from material to material. A strain amplitude of 0.2% was used for all the materials except the O-ring which was tested at a level (5%) more relevant to its structural application.

Application of reduced variables to the shear-storage modulus of the O-ring material is presented in Figure 4. Also shown in this figure is the corresponding curve for the loss modulus. These curves were obtained by horizontally superposing modulus data at different temperatures onto a master frequency curve. The horizontal shift factors, $a_T$, used to superpose the $G'$ data are given in the figure inset. A reference temperature of 1°C was arbitrarily selected, and the individual moduli corrected for the change in thermodynamic reference state using the equation

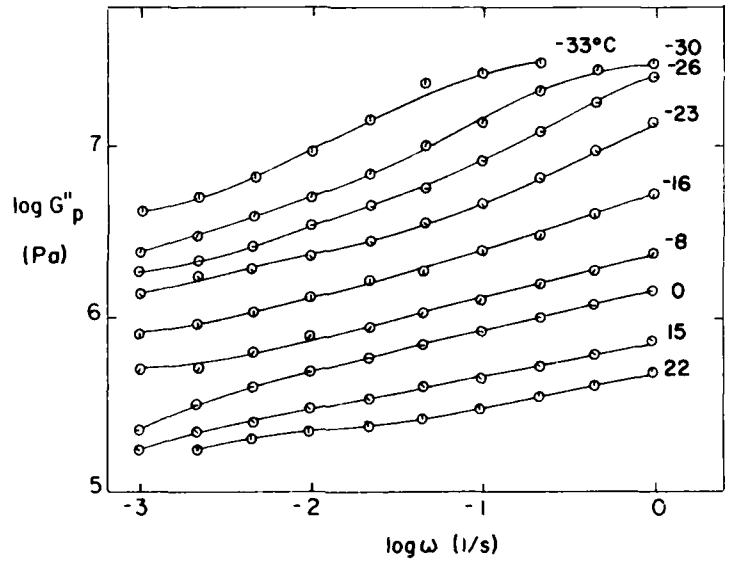


FIG. 3.—Effect of frequency and temperature on the shear loss modulus, $G''$, of the putty. Strain = 0.2%.

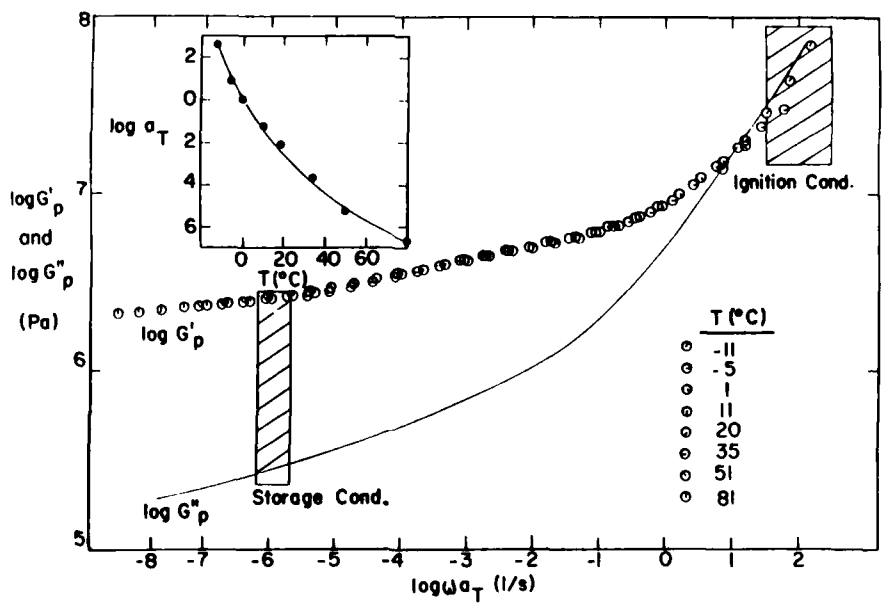


FIG. 4.—Temperature reduced master curves of dynamic moduli for the O-ring material. Reference temperature = 0°C, strain = 5%.

$$G'_p = G'(T_o/T), \tag{5}$$

where $T$ is the test temperature and $T_o$ is the reference temperature.

Figure 4 shows several important features concerning the viscoelastic response of the O-ring material. At low temperatures or high frequencies, $G'$ and $G''$ are approximately equal and their slopes maximize. This temperature/frequency region of the viscoelastic spectrum is commonly termed the transition region[27], referring to the transition of the material from a soft elastomer to, at first a leathery, then a hard glassy solid. As illustrated in this figure, the strain rate of the material during rocket motor ignition conditions corresponds to this transition region. Generally, it is considered good engineering practice not to select materials for structural applications which display this transition region within the expected operational conditions. At higher temperatures, or lower frequencies, Figure 4 shows $G''$ becoming progressively smaller than $G'$, with both curves entering the rubbery plateau region. The loading conditions of the O-ring material during rocket motor storage conditions correspond to the center of this plateau region.

Although the aforementioned complicating features of filled systems make application of reduced variables questionable, the data for each of the other materials were shifted into master curves in an identical fashion to that used for the O-ring material. Data at different temperatures shifted readily; however, some evidence of thermorheologically complex behavior was observed as indicated by slightly different shift coefficients for $G'$ and $G''$. This difference is identical to that previously reported by Adicoff and Lepie[28]. Throughout this paper, the reported shift coefficients are derived from $G'$ for consistency. Figure 5 provides a comparison of the $G'$ and $G''$ master curves for all five materials.

All of the materials in Figure 5 are referenced to 0°C instead of to their individual glass transition temperatures to reduce overlapping of the curves; this explains much of the displacement observed between the curves. Additionally, variations in crosslink density among the materials may account for some of the vertical separations since $G'$ and $G''$ are generally believed to be directly proportional to crosslink density in some regions of the viscoelastic spectrum[13]. Keeping these limitations in mind, the data in Figure 5 may be evaluated as follows.

The vertical separation of these curves appears similar to the reference modulus values presented in Table II. Conditioning the putty with humidity serves a plasticization function, softening the material over the entire data range. As was discussed in Figure 4, each of the curves contains a rubbery plateau and transition region. Additionally, the insulation material displays evidence of a glassy plateau at the high-frequency or low-temperature extreme. In the low-frequency or high-temperature region of the crosslinked elastomers, only the O-ring material appears to approach an equilibrium storage modulus. It is not, however, as distinct as that displayed by an unfilled elastomer. Kelley[6] has discussed the difficulty of measuring equilibrium modulus for highly filled elastomers in terms of gradual dewetting of the binder filler composite structure. This provides an additional relaxation mechanism which masks the rubbery plateau of the polymeric network. This phenomenon may be closely related to the nonlinear viscoelastic response previously discussed, since strain-amplitude dependence is sensitive to frequency[2]. Additional work will be required before these mechanisms are fully understood.

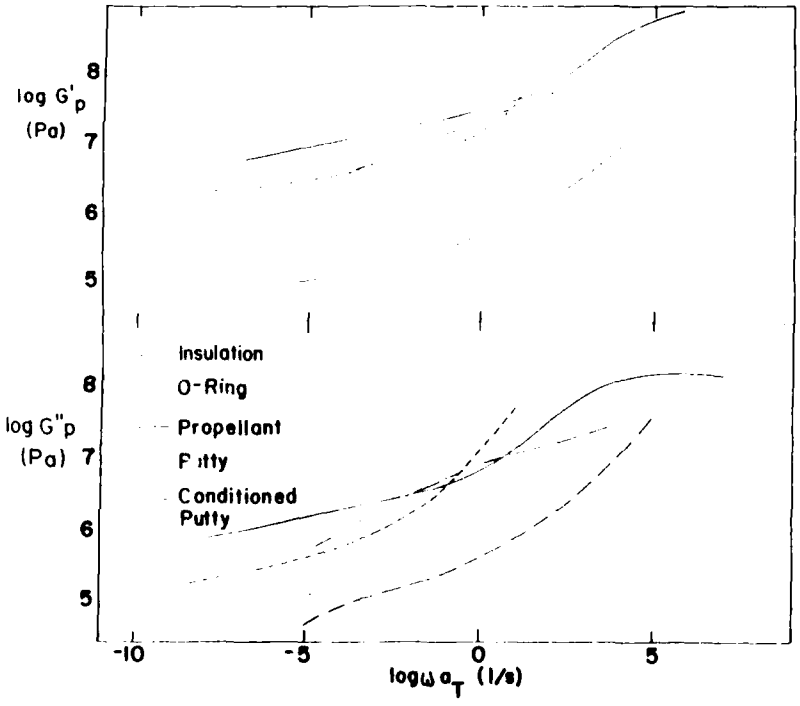


FIG. 5.—Temperature reduced master curves of dynamic moduli, (a) $G'$ and (b) $G''$, for five materials as indicated. Reference temperature = 0°C; strain = 5% for O-ring material, 0.2% for all others.

Table III presents the WLF (Williams, Landel, and Ferry) and free volume constants for the materials investigated. These were determined from the shift factors used to superpose the $G'$ data in Figure 5a. Shift factors for $G''$ data were somewhat

TABLE III

WLF AND FREE VOLUME CONSTANTS

| Material | $T_g$, °C | $C_1$ | $C_2$, deg | $f_g$ | $\alpha$ deg$^{-1}$ · $10^{-4}$ |
|---|---|---|---|---|---|
| "Universal" | — | 17.4 | 51.6 | 0.025 | 4.80 |
| Insulation | 35[a] | 25.5 | 117.2 | 0.017 | 1.45 |
| O-Ring | 16[a] | 16.8 | 73.0 | 0.026 | 3.54 |
| Propellant | 80[a] | 23.5 | 83.9 | 0.018 | 2.20 |
| Putty | 47[b] | 17.2 | 53.5 | 0.025 | 4.73 |
| Conditional putty | 51[b] | 16.5 | 48.6 | 0.026 | 5.43 |

[a] By mechanical testing.
[b] By differential scanning calorimetry.

different but not significant enough to affect any of the conclusions reached. The constants $C_1$ and $C_2$ in this table were determined from the WLF equation[13]

$$-\log a_t = C_1(T - T_g)/[C_2 + (T - T_g)], \tag{6}$$

where $T_g$ is the glass transition temperature of the material. The importance of the WLF coefficients[5], $C_1$ and $C_2$, can be seen through the relationship

$$f_g = B/2.303C_1 \tag{7}$$

and

$$\alpha = f_g/C_2, \tag{8}$$

where $B$ is a constant in the Doolittle equation assumed equal to unity[13], $f_g$ is the fractional free volume at the glass-transition temperature, and $\alpha$ is the thermal coefficient of expansion of the free volume above $T_g$. Use of Equations (6–8) allows the experimentally determined shift factors to be directly related to the physically significant parameters $f_g$ and $\alpha$.

Comparing the experimentally determined WLF and free volume constants in Table III with the "universal" constants determined by averaging the values of a wide variety of polymers[15] leads to several interesting observations. Both the O-ring and putty have a temperature-dependent viscoelastic response which is very close to "universal," while the insulation and propellent differ significantly. As was the case for the modulus values, data in Table III indicate that water acts as a plasticizer for the putty, lowering the glass-transition temperature while increasing the thermal coefficient of free volume expansion. With the exception of the conditioned putty, all the materials have $\alpha$ values that are less than or equal to the "universal" $\alpha$. These low values could be related to the presence of filler in the compounds. Thermal expansion studies by van der Wal and coworkers[5] have shown that increasing amounts of sodium chloride filler result in a linear decrease in $\alpha$. A similar observation was made for carbon-black-filled NR and SBR compounds[29]. This behavior was discussed in terms of a postulated mechanism of filler restricting normal free volume expansion of the binder.

In addition to providing response properties that can be used for structural analysis, the master curves in Figure 5 can be used to calculate all the common viscoelastic functions using well-documented transformations[13]. Of greater relevance to the O-ring, which is required to seal joints in solid rocket motors, preventing the escape of hot gases, these data can be used to obtain mastercurves of resilience. Because O-rings employed in solid rocket motor applications must respond rapidly (strain rate, $\dot{\epsilon} \simeq 0.01\ s^{-1}$) during motor ignition, resilience capability at different operating conditions is an important structural parameter. Resilience, $R$, can be defined as the ratio of energy stored during deformation to the total energy required to produce the deformation[30] and may quantitatively be represented by

$$R = \frac{\xi_s}{\xi_d + \xi_s}, \tag{9}$$

where $\xi_s$ and $\xi_d$ are the energy stored and energy dissipated per unit volume, respectively. These values can be calculated from the dynamic data previously presented through equations developed by Kramer and Ferry[27]. For a single loading

or unloading condition (occurring during one-quarter cycle of a dynamic test) these values are:

$$\xi_s = \gamma^2 G'(\omega) \int_0^{\pi/2} \sin \omega t d \sin \omega t = \tfrac{1}{2}\gamma^2 G'(\omega) \tag{10}$$

and

$$\xi_d = \gamma^2 G''(\omega) \int_0^{\pi/2} \cos^2 \omega t d(\omega t) = (\pi/4)\gamma^2 G''(\omega), \tag{11}$$

where $\omega$ is frequency and $t$ is time. Substituting these expressions into Equation (9) gives

$$R(\omega) = -G'(\omega)/[G'(\omega) + (\pi/2)G''(\omega)]. \tag{12}$$

Figure 6 presents a nomogram of O-ring resilience as a function of time. The conversion to the time axis was accomplished by assuming $t = 1/\omega$. Resilience at a given time and temperature can be extracted from these curves by drawing intersecting lines. Seven parallel curves are shown, each representing a master curve of resilience at a different reference temperature, calculated from Equation (12). The horizontal spacing between these curves increases as temperature decreases. This spacing is directly related to the effects of temperature on molecular free volume as reflected in the horizontal shift factors in the Figure 4 inset.

Data in Figure 6 indicate that the resilience of the O-ring dramatically decreases as $T_g$ is approached. The rubber-to-glass transition region for elastomers usually

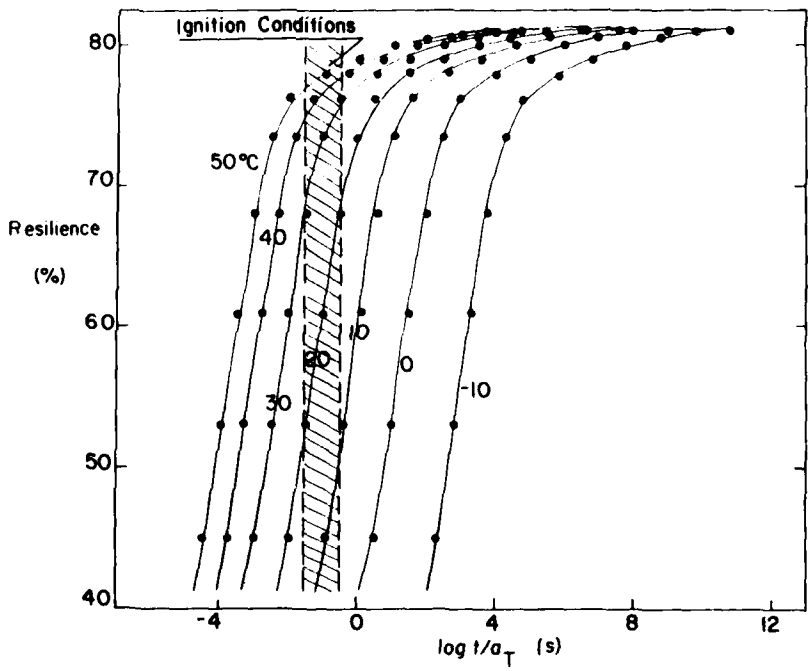


FIG. 6.—Nomogram of calculated O-ring resilience as a function of temperature-reduced time.

begins at approximately $T_g$ + 20°C [13]. Ignition conditions (derived from strain rate) of a typical solid rocket motor are highlighted in the figure. At 20°C and above, the O-ring recovers approximately 70% of its original shape within 100 ms. However, if the temperature is reduced by 20°C, resilience decreases by a factor of two, to less than 35%. Clearly the structural capability of the O-ring varies dramatically within the rubber-to-glass transition region, making its efficacy uncertain at temperatures in this range.

### ADHESIVE FRACTURE

Bond samples consisting of a putty layer sandwiched between two insulation layers were evaluated using a 180° peel test. Adhesive fracture energy was determined as a function of temperature and crack growth rate, as previously described. These results are presented as a master curve of $G_a$ *vs.* temperature-reduced inverse strain rate in Figure 7. Strain rate was estimated from the crack growth rate, $\dot{c}$, using the relationship[31]

$$\dot{\epsilon} = \dot{c}/h, \tag{13}$$

where $h$ is the thickness of the putty layer. No difficulties or irregularities were observed in shifting data at different temperatures. All samples failed cohesively in the putty except at the lowest temperature (−14°C) and highest rates evaluated. Legging of the putty layer was observed in the samples that failed cohesively. This is a common phenomenon of bonded interfaces where some unbroken filaments of the adhesive continue to bridge the gap between the two separating surfaces behind the progressing crack tip[32]. Peel force fluctuations were minimal in this case. However, at the low-temperature and high-rate extremes, peel force fluctuation was

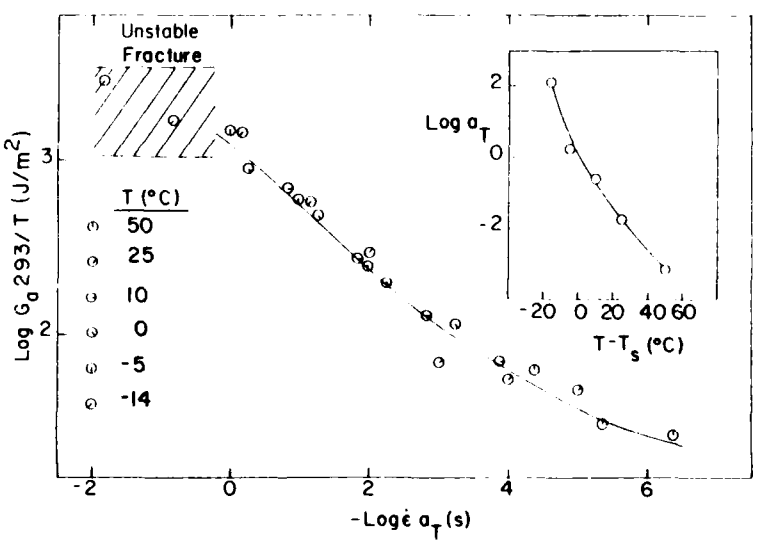


FIG. 7.—Master curves of adhesive fracture energy, $G_a$, for putty/insulation bond as a function of temperature-reduced inverse strain rate. Reference temperature = 0°C.

pronounced, and adhesive failure between putty and insulation was observed. These conditions are illustrated by the hashed region in Figure 7.

The horizontal shift factors used to superpose the adhesive fracture data are given in the figure inset. The WLF equation was used to describe these data with the constants $C_1 = 21.7$ and $C_2 = 103.6°$. Applying Equations (7 and 8) gives an $\alpha$ of $1.93 \times 10^{-4}$ deg$^{-1}$. Comparing these values to those of the insulation and putty in Table III shows that the behavior of the composite joint is intermediate between its two material components. This indicates that the temperature dependency of both the insulation and putty contribute to the overall response of the peel joint. Behavior of this type has been previously described in terms of an effective reference state (related to $T_g$) of the composite joint, determined by a volume rule of additivity normalized for the moduli of the individual components[33].

Fracture of elastomeric materials is usually discussed in terms of its associated dissipative processes[14,20,34-36]. In fact, some researchers have suggested that fracture energy is a second-order material property, derived from viscoelastic dissipation[37,38]. However, quantitative relationships between viscoelastic dissipation and fracture remain a subject of controversy[36]. As discussed above, both the insulation and putty appear to contribute to the overall bond performance. A comparison of the $G_a$ curve in Figure 7 with the $G''$ curves in Figure 5b suggests that the shape of the putty $G''$ curve more closely resembles that of the $G_a$ curve. Correlation between these two curves is shown in Figure 8. This plot shows the shear loss modulus at one decade frequency intervals as a function of the adhesive fracture energy at the corresponding strain rate. Excellent linear correlation exists between these two curves except in the region where unstable fracture, represented by the dashed line, was observed.

The linear relationship between $G_a$ and $G''$ in Figure 8 suggests that the intercept may have physical significance. The slope is not of interest since $G''$ is not the energy term of interest, but only proportional to the energy term of interest, $\xi_d$ [see Equation (11)]. A previous attempt to relate $G''$ to the tear energy of a series of elastomers found that the intercept (fracture energy in the absence of viscoelastic dissipation) could be related to the threshold tear strength[39]. Application of linear regression to the data shown in Figure 8 (without logarithmic transformation of $G_a$ and $G''$) reveals a negative intercept. A possible explanation for this discrepancy is that the contribution of the backing and substrate are not included. Attempts to use $G''$ of the insulation or combine the loss functions of the insulation and putty in proportion to their effect on $\alpha$ were unsuccessful. Other possibilities are that different effects may occur in various regions of the viscoelastic spectrum, or that the nonlinear viscoelastic behavior previously discussed influences the correlation.

Practical use of the putty in solid rocket motors involves laying up several layers of putty before bonding to the insulation. Consequently, different thicknesses are often used. Gent and Hamed[40,41] have evaluated the effects of interlayer thickness on bond strength and found that at small thicknesses (less than 1 mm), adhesive strength was linearly related to thickness. However, at greater thicknesses, bond strength was found to be independent of the amount of adhesive. Similar results were obtained for the insulation/putty bond in this study. As shown in Figure 9, $G_a$ determined over a range of temperatures is dependent on $h$ below approximately 1 mm. At greater thicknesses, $G_a$ appears to decrease slightly with increasing amounts of putty, especially at lower test temperatures. The nature of this decrease is un-

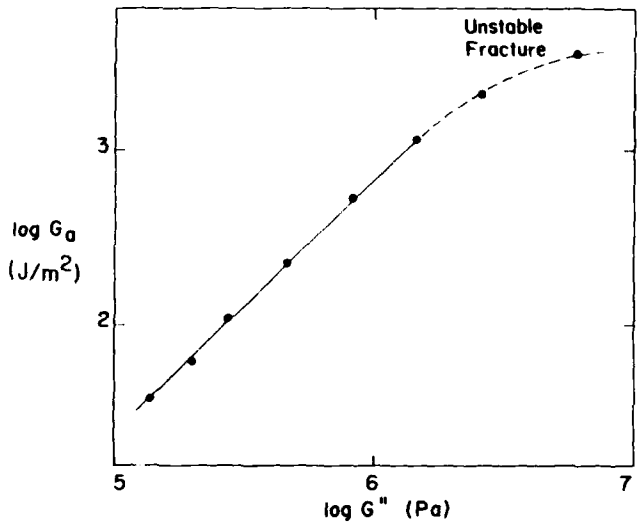


FIG. 8.—Correlation of adhesive fracture energy of insulation/putty bond with shear loss modulus of putty at one time decade intervals.

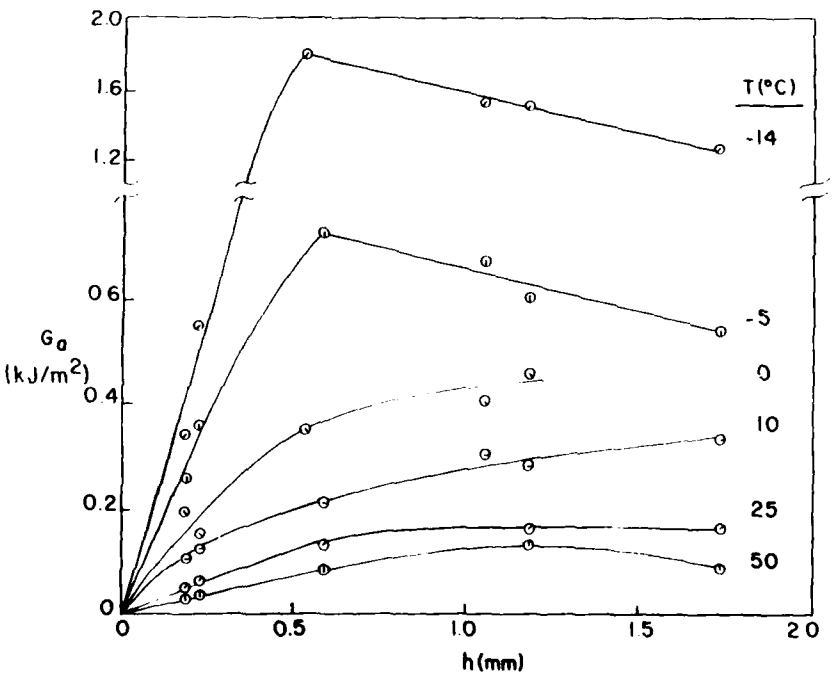


FIG. 9.—Effect of putty thickness, $h$, on adhesive fracture energy of insulation/putty bond at selected temperature as indicated.

known. Attempts to account for this decrease in terms of a change in strain rate in the thicker putty samples were unsuccessful.

Gent and Hamed[40,41] have argued that the effect of interlayer thickness on bond strength is related to the amount of energy dissipation and the size of the region around the crack tip into which this energy can be dissipated. Consequently, at thicknesses above a critical value, $G_a$ is believed to level off because the propagating crack can no longer utilize the increased volume to dissipate energy. Below this critical value, however, the slope of the $G_a$ *vs.* $h$ curve should be related to an energy dissipation function. Since $G''$ is proportional to the energy dissipated per unit volume [see Equation (11)], it should be possible to correlate $G''$ with the initial slope, $r$, of the curves in Figure 9. This hypothesis is tested in Figure 10. A strong linear relationship is shown in this figure, suggesting that the dependence of $G_a$ on thickness is a function of the energy dissipated within the adhesive layer. Generation of this plot was accomplished by determining $r$ from the slope of the three smallest thickness values in Figure 9 for each temperature. With the exception of 0 and 10°C, these lines all pass through the origin of Figure 9 within experimental error. It should also be noted that the slopes of the curves at 0 and 10°C showed the greatest deviation from the best fit line in Figure 10.

Because of its high tack, the putty is stored and applied at low temperatures. One of the primary criteria for good bond strength in an elastomeric joint is molecular interdiffusion between the two contacted surfaces[42-44]. Diffusion in polymers is related to free volume[15], and hence to temperature. As a practical result, bond formation in the insulation/putty joint will be slower at lower temperatures. Although diffusion is discussed as an important contribution to bond strength, most adhesive fracture studies focus on the bond after an apparent equilibrium has been achieved. An identical approach was used to generate the data in Figure 7, *i.e.*, the

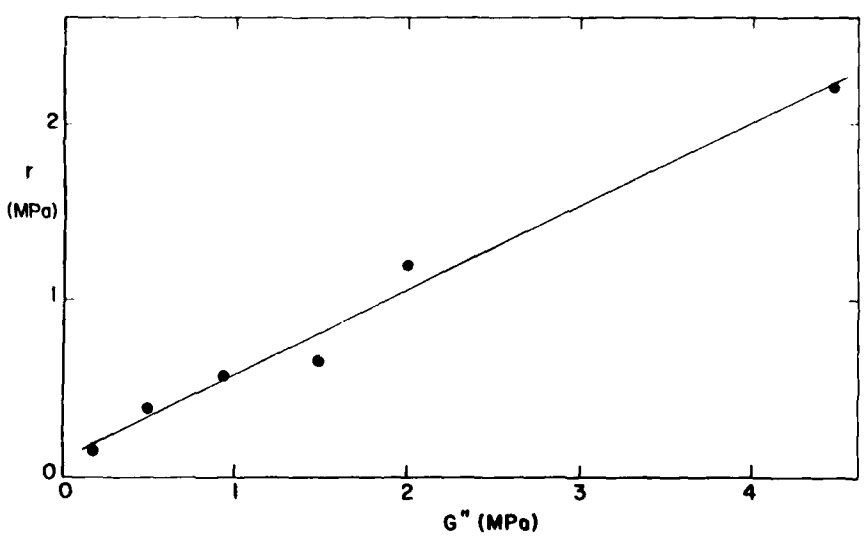


FIG. 10.—Correlation of initial slope, $r$, from putty thickness *vs.* adhesive fracture energy of insulation/putty with the shear loss modulus of the putty.

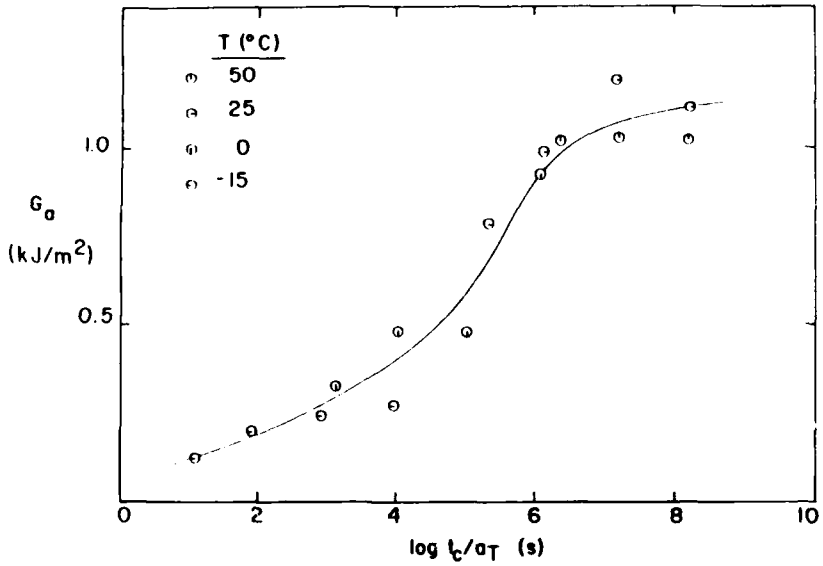


FIG. 11.—Master curve of adhesive fracture energy at 0°C and rate of 5 cm/min, as a function of temperature reduced contact time, $t_1$. Reference temperature = 0°C.

joint was tested at different temperatures and rate conditions after an apparent equilibrium contact time had been achieved. Alternately, the composite joint can be tested at constant temperature and rate while varying contact temperature and time. This later approach has the advantage of being more relevant to the diffusion process of interest. Figure 11 presents data for the insulation/putty bond evaluated in this fashion. Samples were contacted at four different temperatures for periods up to 15 days. $G_a$ was measured at a constant rate at 0°C. This test temperature was chosen to minimize diffusion during the brief (relative to total contact time) test period.

Data in Figure 11 are given as a master curve of adhesive fracture energy with respect to temperature-reduced contact time. Data scatter was large, so shifting was accomplished using the factors previously established for the insulation/putty bond, given in Figure 7. Additional work will be necessary to fully validate the application of reduced variables to contact time, however, several promising results are available from this treatment at this time. At low temperatures of short contact times, $G_a$ plateaus at approximately 0.2 kN/m. This region is clearly associated with minimal interdiffusion of polymer chain segments. Bond strength is enhanced as contact time increases. An apparent equilibrium strength of 1.2 kN/m is reached at long reduced-contact times. Between these two extremes, an S-shaped curve is observed. Similarly shaped curves have been reported for plastic/rubber joints formed over a broad range of temperatures[45], although the relationship between contact time and temperature was not addressed. Behavior of this type would be expected from a diffusion-controlled process. Bond strength increases rapidly with time and temperature in this intermediate range. For example, at the putty storage and application

temperatures used in solid rocket motors, 0°C, full bond strength is not achieved for approximately 12 days. At room temperature, this strength level is achieved in about 30 min. It is this intermediate region which is critical to understanding the diffusion mechanism and bond strength formation. The shape of this curve, and especially the slope, in this intermediate range is somewhat unclear due to the limited number of data points. Future research will be required to fully define bond strength formation in this intermediate range.

## SUMMARY

The viscoelastic response of four highly-filled elastomers has been investigated. Small deformation dynamic testing of these materials reveals thay they are nonlinear viscoelastic, as well as thermorheologically complex. Nonlinear viscoelastic behavior was observed as a pronounced strain dependence in the range of 0.1 to 10%. The degree of this nonlinear response was quantified through a constitutive equation containing a single nonlinear factor; resultant nonlinear factors for the various materials were compared and evaluated. Thermorheologically complex behavior was displayed by slightly different shift coefficients to superpose $G'$ and $G''$ data. An approach for calculating material resilience from the viscoelastic data was also developed and a nomographic technique presented for its application.

A composite adhesive joint, consisting of two layers of a filled NBR compound bonded together by a filled putty interlayer, was also studied. It was found that both the adhesive fracture energy and the effect of interlayer thickness could be related to the loss modulus of the putty interlayer. Finally, the effect of contact time on bond strength was evaluated and results presented as a master curve of adhesive fracture energy *vs.* temperature-reduced contact time.

## REFERENCES

[1] A. R. Payne, *J. Appl. Polym. Sci.* **7**, 873 (1963).
[2] A. R. Payne and R. E. Whittaker, RUBBER CHEM. TECHNOL. **44**, 440 (1971).
[3] A. I. Medalia, RUBBER CHEM. TECHNOL. **51**, 437 (1978).
[4] R. F. Landel and T. L. Smith, *J. Am. Rocket Soc.* **31**, 599 (1961).
[5] C. W. van der Wal, H. W. Bree, and F. R. Schwarzl, *J. Appl. Polym. Sci.* **9**, 2143 (1965).
[6] F. N. Kelley, in "Propellants Manufacture, Hazards and Testing," C. Boyers and K. Klager, Eds., American Chemical Society, Washington D.C., 1969.
[7] T. B. Lewis and L. E. Nielsen, *J. Appl. Polym. Sci.* **14**, 1449 (1970).
[8] B. L. Lee and L. E. Nielsen, *J. Compos. Mater.* **6**, 136 (1972).
[9] A. E. Oberth, RUBBER CHEM. TECHNOL. **40**, 1337 (1967).
[10] A. N. Gent, *J. Appl. Polym. Sci.* **18**, 1397 (1974).
[11] A. R. Payne, in "Reinforcement of Elastomers," G. Kraus, Ed., Wiley, New York, 1965.
[12] A. N. Gent and H. J. Kim, RUBBER CHEM. TECHNOL. **51**, 35 (1978).
[13] J. D. Ferry, "Viscoelastic Properties of Polymers," Third Edition, Wiley, New York, 1980.
[14] F. R. Eirich and T. L. Smith, in "Fracture: An Advanced Treatise, Vol. 7," H. Liebowitz, Ed., Academic Press, New York, 1972.
[15] G. Kraus, in "Science and Technology of Rubber," F. R. Eirich, Ed., Academic Press, New York, 1978.
[16] L. E. Nielsen, "Mechanical Properties of Polymers and Composites, Vol. 2," Dekker, New York, 1974.
[17] R. A. Dickie, in "Polymer Blends, Vol. 1," D. R. Paul and S. Newman, Eds., Academic Press, New York, 1978.
[18] F. H. Wetzel, in "Handbook of Adhesives," I. Skeist, Ed., Reinhold, New York, 1962.
[19] A. E. Hicks, V. E. Chirico, and J. D. Ulmer, RUBBER CHEM. TECHNOL. **45**, 26 (1972).
[20] A. N. Gent and A. J. Kinloch, *J. Polym. Sci. Part A-2* **9**, 659 (1971).
[21] K. E. Gui, C. S. Wilkinson, and S. D. Gehman, *Ind. Eng. Chem.* **44**, 720 (1952).

[22] J. D. Ulmer, V. E. Chirico, and C. E. Scott, RUBBER CHEM. TECHNOL. **46**, 897 (1973).
[23] A. K. Sircar and T. G. Lamond, RUBBER CHEM. TECHNOL. **48**, 79 (1975).
[24] A. R. Payne, *J. Appl. Polym. Sci.* **8**, 2661 (1964).
[25] W. P. Fletcher and A. N. Gent, *Trans. Inst. Rubber Ind.* **29**, 266 (1953).
[26] A. R. Payne, R. E. Whittaker, and J. F. Smith, *J. Appl. Polym. Sci.* **16**, 1191 (1972).
[27] O. Kramer and J. D. Ferry, in "Science and Technology of Rubber," F. R. Eirich, Ed., Academic Press, New York, 1978.
[28] A. Adicoff and A. Lepie, *J. Appl. Polym. Sci.* **14**, 953 (1970).
[29] R. G. Stacer, E. D. von Meerwall, and F. N. Kelley, RUBBER CHEM. TECHNOL. **58**, 913 (1985).
[30] F. S. Conant, in "Rubber Technology, 2nd Edition," M. Morton, Ed., Van Nostrand-Reinhold, New York, 1973.
[31] A. N. Gent and R. P. Petrich, *Proc. R. Soc. London Ser. A* **310**, 433 (1969).
[32] D. H. Kaelble, *Trans. Soc. Rheol.* **9**, 135 (1965).
[33] H. L. Stacer and R. G. Stacer, presented at a meeting of the Adhesion Society, Hilton Head Island, South Carolina, February 9-12, 1986.
[34] L. Mullins, *Trans. Inst. Rubber Ind.* **35**, 213 (1959).
[35] E. H. Andrews, *J. Mater. Sci.* **9**, 887 (1974).
[36] A. J. Kinloch and R. J. Young, "Fracture Behavior of Polymers," Applied Science, London, 1983.
[37] H. K. Mueller and W. G. Knauss, *Trans. Soc. Rheol.* **15**, 217 (1971).
[38] J. Glucklich and R. F. Landel, *J. Appl. Polym. Sci.* **20**, 121 (1976).
[39] R. G. Stacer, Ph.D. Dissertation, University of Akron, 1986.
[40] A. N. Gent and G. R. Hamed, *Polym. Eng. Sci.* **17**, 462 (1977).
[41] A. N. Gent and G. R. Hamed, *Plast. Rubber: Mater. Appl.* **3**(1), 17 (1978); RUBBER CHEM. TECHNOL. **51**, 354 (1978).
[42] G. R. Hamed, RUBBER CHEM. TECHNOL. **54**, 576 (1981).
[43] S. Wu, "Polymer Interface and Adhesion," Dekker, New York, 1982.
[44] M. D. Ellul and A. N. Gent, *J. Polymer Sci. Polym. Phy. Ed.* **22**, 1953 (1984).
[45] L. F. Plisko, V. V. Lavrentyev, V. L. Vakula, and S. S. Voyutskii, *Polym. Sci. USSR*, **14**, 2501 (1972).